An adaptive control scheme for flexible power point tracking in photovoltaic systems

Dehghani Tafti, Hossein; Sangwongwanich, Ariya; Yang, Yongheng; Pou, Josep; Konstantinou, Georgios; Blaabjerg, Frede

2018

Dehghani Tafti, H., Sangwongwanich, A., Yang, Y., Pou, J., Konstantinou, G., & Blaabjerg, F. (2018). An adaptive control scheme for flexible power point tracking in photovoltaic systems. IEEE Transactions on Power Electronics, In press. doi:10.1109/TPEL.2018.2869172

https://hdl.handle.net/10356/88878

https://doi.org/10.1109/TPEL.2018.2869172

An Adaptive Control Scheme for Flexible Power Point Tracking in Photovoltaic Systems

Hossein Dehghani Tafti[1*], *Member, IEEE,* Ariya Sangwongwanich[2], *Student Member, IEEE,*
Yongheng Yang[2], *Senior Member, IEEE,* Josep Pou[1], *Fellow, IEEE,*
Georgios Konstantinou[3], *Senior Member, IEEE,* Frede Blaabjerg[2], *Fellow, IEEE,*
[1]School of Electrical and Electronic Engineering, Nanyang Technological University, Singapore.
[2]Department of Energy Technology, Aalborg University, Denmark.
[3]School of Electrical Engineering and Telecommunications, University of New South Wales, Australia.
[*] hossein002@e.ntu.edu.sg

Abstract

One of the major concerns associated with the increasing penetration of grid-connected photovoltaic (PV) power plants is the operational challenges (e.g., overloading and overvoltage), imposed due to the variability of PV power generation. A flexible power point tracking (FPPT), which can limit the PV output power to a specific value, has thus been defined in grid-connection regulations to tackle some of the integration challenging issues. However, the conventional FPPT algorithm based on the perturb and observe method suffers from slow dynamics. In this paper, an adaptive FPPT algorithm is thus proposed, which features fast dynamics under rapidly changing environmental conditions (e.g., due to passing clouds), while maintaining low power oscillations in steady-state. The proposed algorithm employs an extra measured sampling at each perturbation to observe the change in the operating condition (e.g., solar irradiance). Afterwards, the voltage-step is adaptively calculated following the observed condition (e.g., transient or steady-state) in a way to improve the tracking performance. Experimental results on a 3-kVA grid-connected single-phase PV system validate the effectiveness of the proposed algorithm in terms of fast dynamics and high accuracy under various operational conditions.

Index Terms

Adaptive voltage-step calculation, constant power generation, photovoltaic systems, photovoltaic panel power-voltage curve, voltage reference calculation

NOMENCLATURE

p_{ref}	Power reference.
$v_{p\text{-}ref}$	Corresponding voltage to the constant power reference.
$p_{pv}(k)$	Instantaneous PV power at calculation time-step k.
dp_1	PV power change between $t=(k-1)T$ and $t=(k-1/2)T$.
dp_2	PV power change between $t=(k-1/2)T$ and $t=kT$.
dp^*	PV power error between p_{ref} and $p_{pv}(k)$.
dv	PV voltage change between $t=(k-1)T$ and $t=kT$.

T_{step}	Calculation time-step.
V_{step}	Voltage-step.
$V_{step\text{-}b}$	Optimal voltage-step for the MPPT operation.
$V_{step\text{-}tr}$	Transient voltage-step.
V_{ref}	PV panel voltage reference.
k_1, k_2	Voltage-step calculation proportional gains.
α	Parameter for differentiating operation modes.
dp_{th}	Threshold power.
$Thr.$	Threshold dp/dv.
p_{mpp}	PV panel maximum power.
v_{mpp}	PV panel maximum power-point voltage.
i_{mpp}	PV panel maximum power-point current.
i_{mpp}	PV panel maximum power-point current.
FF	PV panel filling factor.
v_{dc}	dc-bus voltage.
C_{pv}	PV-side capacitor.
C_{dc}	dc-link capacitor.
f_{sw}	Converter switching frequency.
v_g	Grid voltage.
i_g	Grid current.
$Irr.$	Solar irradiance.
$Temp.$	Temperature.
$T.E.$	Tracking error.
p_{avai}	Instantaneous maximum available power from the PV panels.

I. Introduction

The increasing installation of grid-connected photovoltaic power plants (GCPVPPs) may lead to overvoltages in the power infrastructure during peak power generation periods (e.g., noon time in a day), if the grid power capacity remains the same [1]. In order to tackle potential challenging issues for the power system, grid codes and/or standards are continuously updated [2], [3]. For instance, the Danish grid code requires that a GCPVPP with a power output above 11 kVA should be able to limit the output power to a certain constant value if required [2]. By limiting the power output of the GCPVPP, the additional available power can be used to provide ancillary functions, such as frequency support [2]. Furthermore, the power limiting control (also known as constant power generation) [1], [4], [5], power reserve control [6], and power ramp-rate control [7] requirements are imposed by various grid codes on GCPVPPs. Therefore, the existing maximum power point tracking algorithms in GCPVPPs, should be replaced by flexible power point tracking (FPPT) algorithms in GCPVPPs in order to comply with these demands.

In the past, the focus of most research studies in the literature was the maximum power point tracking (MPPT) from PV strings to increase the overall power conversion efficiency and energy utilization [8]–[15]. In addition to the conventional MPPT algorithms, like perturb & observe (P&O) and incremental conductance (I.C.) [8], several advanced algorithms like model-predictive [9], particle swarm optimization method [14] and dual-Kalman filter method [15] are also introduced to extract the maximum power from PV strings. Furthermore, the operation of PV strings under partial shading conditions is considered in [13]. With the introduction of FPPT requirements, several FPPT algorithms have also been introduced for different configurations of GCPVPPs. There are mainly two categories of methods to achieve the FPPT operation:

i) Modifying the dc-dc converter controller in two-stage or dc-ac inverter controller (e.g., Proportional Integral - PI controller) in single-stage GCPVPPs [16]–[24]. The fundamentals of the FPPT are introduced in [16]–[20] with focus on stability issues. A voltage reference calculation method is also introduced in [18], [21], based on the P&O algorithm to calculate the voltage reference related to the required active power. However, moving the operation point to the right-side of the maximum power point (MPP) reduces the robustness of these algorithms, as the operation point may go beyond the open-circuit voltage of the PV panel under fast irradiance reductions. These algorithms apply multi-mode operations to regulate the output power of the PV panels. Clearly, the controller initialization during the operational mode transitions is required and thus slow dynamics are observed.

ii) Adjusting the voltage reference of PV strings per the required power reference according to the power-voltage (P-V) characteristics of the PV panels [1], [4]–[6], [25]. Such approaches do not require any modifications in the dc-dc or dc-ac converter controllers.

Since the second category of FPPT algorithms do not require any changes in the controllers and can achieve fast dynamics, they are chosen in this study for the generation of constant power from GCPVPPs. These algorithms perform well during constant environmental conditions (e.g., irradiance and temperature). However, the power and voltage characteristic of the PV arrays can vary considerably due to environmental changes. Thus, the previous solutions can encounter issues in the calculation of the voltage reference under rapid irradiance changes. Several studies are available in the literature to enhance the operation of MPPT algorithms during rapid environmental changes [26]–[28]. In that case, the performance of FPPT algorithms can be highly affected by environmental condition changes, especially when the operating point is far away from the MPP, because:

- MPPT operating range is narrow around the MPP, while the FPPT operating range covers the entire region of the P-V curve. Therefore, it is more challenging to adapt the control parameters according to the environmental conditions.
- The impact of environmental changes on the PV power during the FPPT operation could be more pronounced compared to the MPPT operation, because the change of the voltage during FPPT has greater impact on the power compared to the MPPT operation.

Furthermore, it is not only environmental changes that can influence the FPPT operation, but also sudden changes of the desired constant power reference (p_{ref}), due to the grid requirements. Hence, the FPPT operation under transients is more challenging compared to the MPPT operation. However, this has not been addressed in the

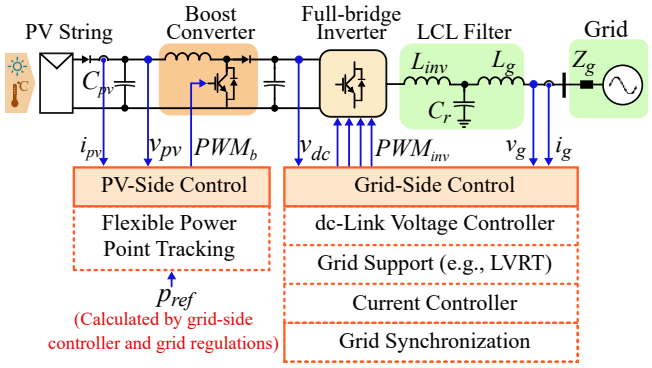

Fig. 1. Circuit configuration and overall control structure of a two-stage GCPVPP.

literature yet.

In light of the above, this paper proposes an adaptive FPPT algorithm for GCPVPPs. The proposed algorithm is an adaptation of the P&O method considering the P-V characteristics of PV panels. The main contributions of the proposed algorithm in this paper are:

- The key contribution is the proposed adaptive voltage-step calculation strategy for a novel FPPT algorithm, which can achieve fast dynamics during *transients*, and low power osculations in steady-state. In the proposed algorithm, the operation mode of the converter and the current operation point of the PV panel are considered in the calculation of the voltage-step in each calculation step. This feature adaptively adjusts the voltage-step in order to enhance the transient and steady-state performances.
- Furthermore, the proposed algorithm is highly robust to fast environmental changes. An extra sampling is used in the proposed controller to differentiate the effect of the intentional voltage changes in the P&O algorithm from environmental changes on the PV panel power. By doing so, wrong movements of the operation point under rapid changing conditions can be avoided.

The proposed FPPT algorithm in this paper can also be used to extract the maximum power from the PV strings, while it is able to limit the PV power to a required value upon demands. While the proposed algorithm achieves fast dynamics during the power-limiting operation mode, it can obtain similar performance when operating in the MPPT mode as the conventional MPPT algorithms. The calculation time-step is fixed for all operational modes, which reduces the complexity of the controller design for different operation states. Additionally, the proposed adaptive FPPT algorithm is able to move the operation point of the PV panel to the right- or left-side of the MPP. It can be implemented in both single- and two-stage GCPVPPs. The performance of the proposed algorithm is evaluated on a 3-kVA two-stage single-phase GCPVPP, as shown in Fig. 1. The two-stage GCPVPP system consists of a grid-connected full-bridge inverter, which provides the grid connection requirements. The dc-dc boost converter provides the FPPT control for the system, while the required power reference (p_{ref}) is calculated from the grid-side controller. The detailed description of this configuration can be found in [6].

The remaining of the paper is organized as following. The principles of the proposed adaptive FPPT algorithm are described in Section II. The detailed explanation of the proposed adaptive FPPT algorithm, including the proposed

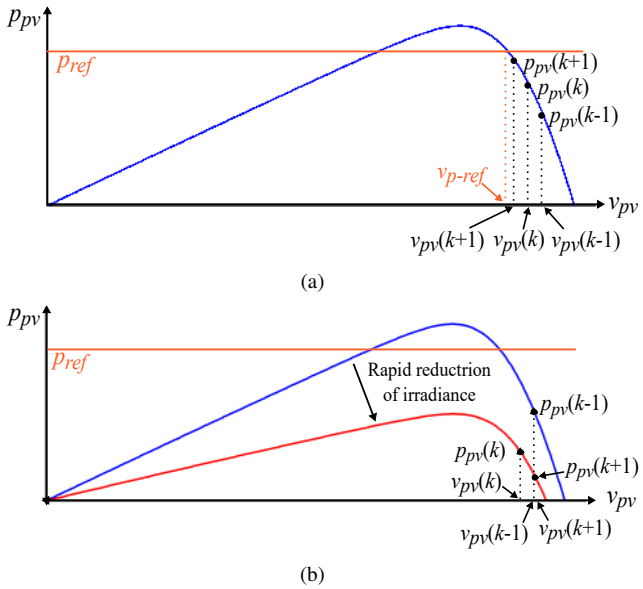

Fig. 2. Effect of the voltage-reference change of the PV panels during: (a) Steady-state environmental condition and (b) rapid irradiance changes.

adaptive voltage-step calculation method, is provided in Section III. The experimental results are presented and discussed in Section IV. Finally, concluding remarks are given in Section V.

II. Principles of the Adaptive FPPT Algorithm

The control objective of the FPPT algorithm is to regulate the output power of the PV system to be constant at a certain set-point. Conventionally, the P&O-based FPPT algorithm, which intentionally perturbs the PV voltage away from the MPP to reduce the output power, is employed as illustrated in Fig. 2(a). According to the effect of the voltage perturbation on the PV output power, the next voltage reference is determined. As illustrated in Fig. 2(a), the PV voltage is $v_{pv}(k-1)$ at $t=(k-1)T$, with k indicating the k^{th} sampling and T being the sampling period. The voltage reference is then changed to $v_{pv}(k)$ at $t=(k-1)T$ and the controller regulates the PV voltage to this value at $t=kT$. Accordingly, the instantaneous power of the PV panel changes from $p_{pv}(k-1)$ to $p_{pv}(k)$. In this condition, a negative voltage change, i.e., $\Delta v_{pv}=v_{pv}(k)-v_{pv}(k-1)<0$, results in a positive power change, i.e., $\Delta p=p_{pv}(k)-p_{pv}(k-1)>0$. Based on the signs of Δv and Δp, the FPPT algorithm decides another voltage decrement in this calculation-step, leading to an increase of the PV power, closer to the power reference (p_{ref}), as shown in Fig. 2(a). Under a constant or slow changing solar irradiance condition, the change in the PV power is mainly induced by the perturbation of the CPG algorithm. Thus, the P&O CPG algorithm can accurately regulate the PV power according to the set-point.

However, under a fast reduction of irradiance, the above process can result in large tracking errors, which is demonstrated in Fig. 2(b). As observed in Fig. 2(b), the same scenario has been applied and a voltage decrement is imposed by the FPPT algorithm at $t=(k-1)T$. A fast reduction of the irradiance occurs during the time interval between $t=(k-1)T$ and $t=kT$. The absolute value of the power reduction due to the decrease of irradiance is larger than the absolute value of the power increment due to the change of the PV voltage. In other words, the

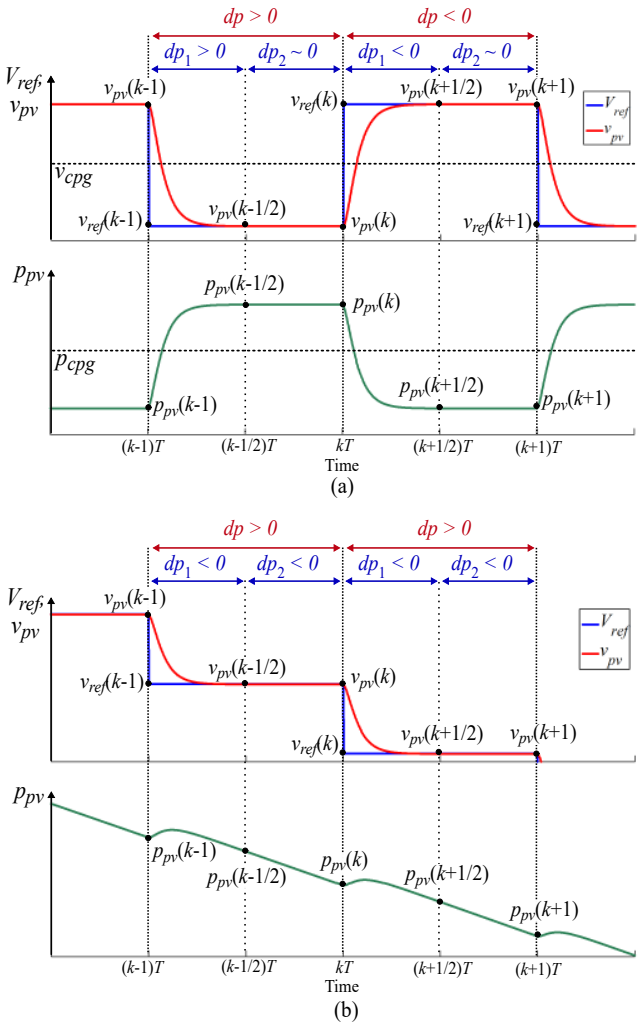

Fig. 3. Extra measurements between consecutive calculation-steps (top: PV voltage, bottom: PV power): (a) Steady-state environmental condition and (b) rapid irradiance changes.

change in the PV power during the perturbation is imposed by the sudden change in the solar irradiance condition. Hence, it will result in a negative change of Δp and the conventional FPPT algorithm may make a wrong decision for the next perturbation, as it can be seen in Fig. 2(b).

The voltage and power curves of the PV panels during FPPT operation in steady-state are illustrated in Fig. 3. It can be seen in Fig. 3 that the operation point oscillates around the power reference p_{ref} in steady-state. The corresponding voltage at p_{ref} is referred to $v_{p\text{-}ref}$, as illustrated in Fig. 2(a). At $t = (k-1)T$, the voltage reference calculation algorithm sets a new voltage reference to $v_{ref}(k-1)$, as shown in Fig. 3(a). An extra measurement is performed to measure the PV voltage and power at $t = (k-1/2)T$. The controller is then designed to regulate the PV voltage v_{pv} in half a sampling period $T/2$. Consequently, the PV voltage v_{pv} is regulated to its reference value (i.e., $v_{ref}(k-1)$) at $t = (k-1/2)T$. The PV output power (p_{pv}) increases to $p_{pv}(k-1/2)$. Between $t = (k-1/2)T$ and $t = kT$, the voltage reference is not changed through the voltage reference calculation algorithm. Therefore, the PV output power p_{pv} remains constant during this period.

According to the above discussions, two parameters are defined in order to detect environmental changes (irradiation and temperature). The first parameter dp_1 calculates the PV power change between $(k-1)T$ and $(k-1/2)T$, and it is given as

$$dp_1 = p_{pv}(k-1/2) - p_{pv}(k-1). \tag{1}$$

During steady-state environmental conditions, dp_1 shows the power change due to the voltage reference perturbation. The PV power change dp_2 between $(k-1/2)T$ and kT is defined as

$$dp_2 = p_{pv}(k) - p_{pv}(k-1/2). \tag{2}$$

Clearly, in steady-state, i.e., constant solar irradiance condition dp_2 is close to zero, since the PV voltage reference is not changed between $(k-1/2)T$ and kT. A relatively large value of dp_2 shows that environmental condition changes are occurring.

The effect of rapid irradiance changes on the above parameters is illustrated in Fig. 3(b). The current operation point of the PV panel in this case study is kept to the same operation point as in Fig. 3(a). However, a rapid linear reduction of the irradiance is considered. The voltage reference at $t = (k-1)T$ is set to $v_{ref}(k-1)$, while the PV power p_{pv} decreases to $p_{pv}(k-1/2)$ at $t = (k-1/2)T$ due to the reduction of the irradiance. Between $t = (k-1/2)T$ and $t = kT$, the PV power p_{pv} decreases. However, the voltage reference is not changed during this period. Consequently, dp_1 is negative in this condition, while positive in steady-state. Furthermore, dp_2 is also negative with a relatively large amplitude, indicating the case of environmental condition changes, although it is close to zero in steady-state.

It is noted that dp_1 includes the information of the power change, which is due to the combination of the effect of irradiation changes and intentional voltage reference changes. The use of the parameter dp_1 in the voltage reference calculation can move the operation point to a wrong direction under environmental changes. Thus, the following parameter is defined to separate the effect of the environmental changes from the effect of the intentional voltage reference changes as

$$dp = dp_1 - dp_2 \tag{3}$$

The change of environmental parameters (irradiation and temperature) is assumed to be linear in one calculation time-step. Any changes in the environmental parameters result in changing the PV power. By assuming the linear change of environmental changes in one calculation time-step, its effect on the PV power for dp_1 is equal to dp_2. Because dp is the difference of dp_1 and dp_2, the effect of environmental changes on the parameter dp is eliminated. As a result, the parameter dp only includes the information about the PV power changes due to the intentional voltage reference perturbations from the controller. In this way, the voltage reference calculation algorithm does not track a wrong direction under rapidly changing environmental conditions.

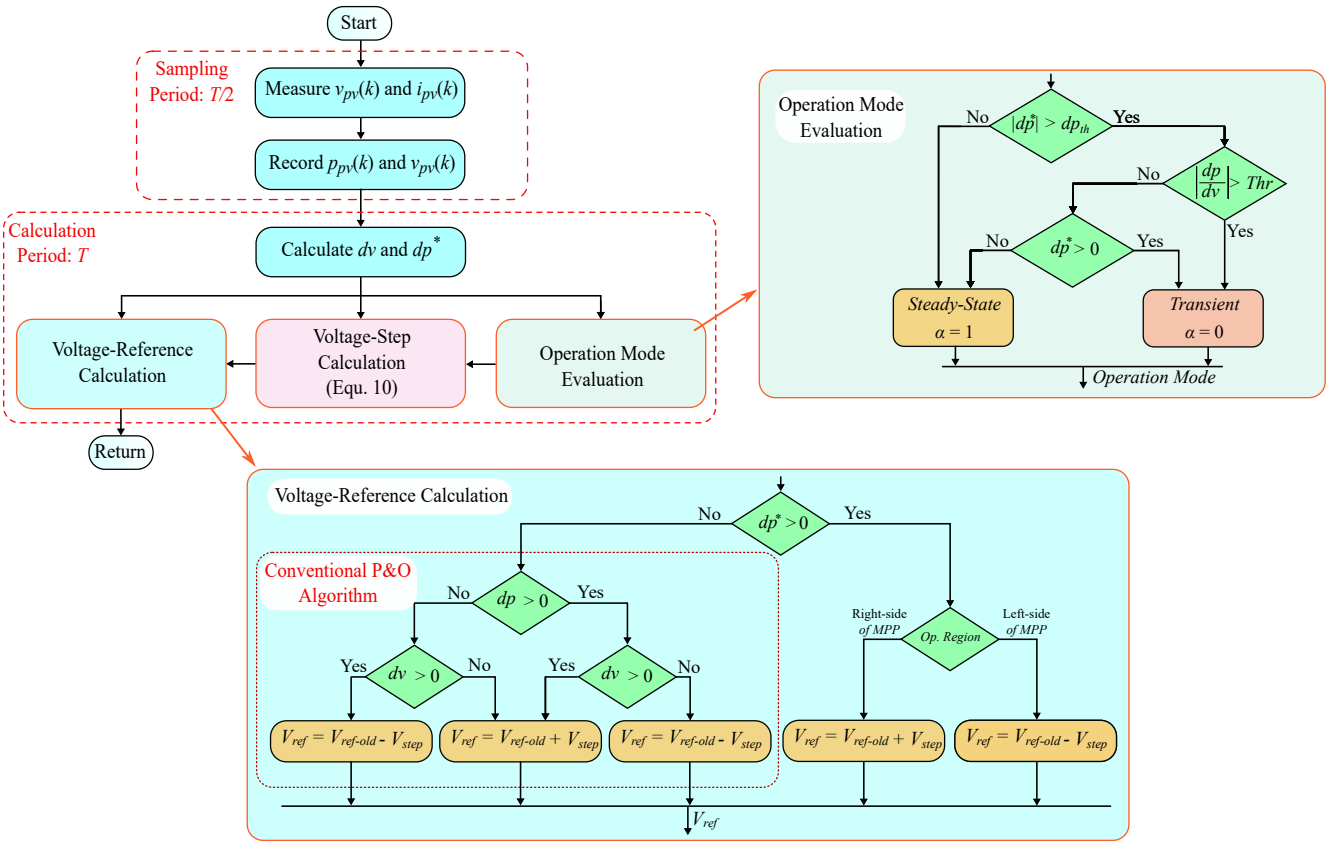

Fig. 4. Block diagram of the proposed adaptive constant power generation algorithm in GCPVPPs.

III. Proposed Adaptive Flexible Power Point Tracking Algorithm

The block diagram of the proposed adaptive FPPT algorithm is illustrated in Fig. 4. The parameters v_{pv} and p_{pv} are measured with a sampling period of $T/2$. It is noted that this extra sampling does not increase the computational complexity of the algorithm. It just requires an extra interrupt for sampling the input measurements. The proposed adaptive FPPT algorithm consists of three parts, which are performed with a calculation period T. Firstly, the operation mode of the PV system is identified as transient or steady-state. This is required to achieve fast dynamics during transient and low power oscillations in steady-state modes. The output of the "operation mode evaluation" block is used as the entry to the "voltage-step calculation" block. Subsequently, the adaptive voltage-step calculation algorithm is implemented to calculate the voltage-step according to the operation mode and PV power change parameters, as defined previously. The calculated voltage-step value by this block is used as the entry to the "voltage reference calculation" block to determine the PV voltage reference for the regulation of the PV power to its reference value. All the calculations of these blocks are implemented in one calculation period of T. The implementation of these parts is presented in detail in the following sections. In the proposed algorithm, the PV voltage change dv between the current and previous calculation-steps is calculated as

$$dv = v_{pv}(k) - v_{pv}(k-1). \tag{4}$$

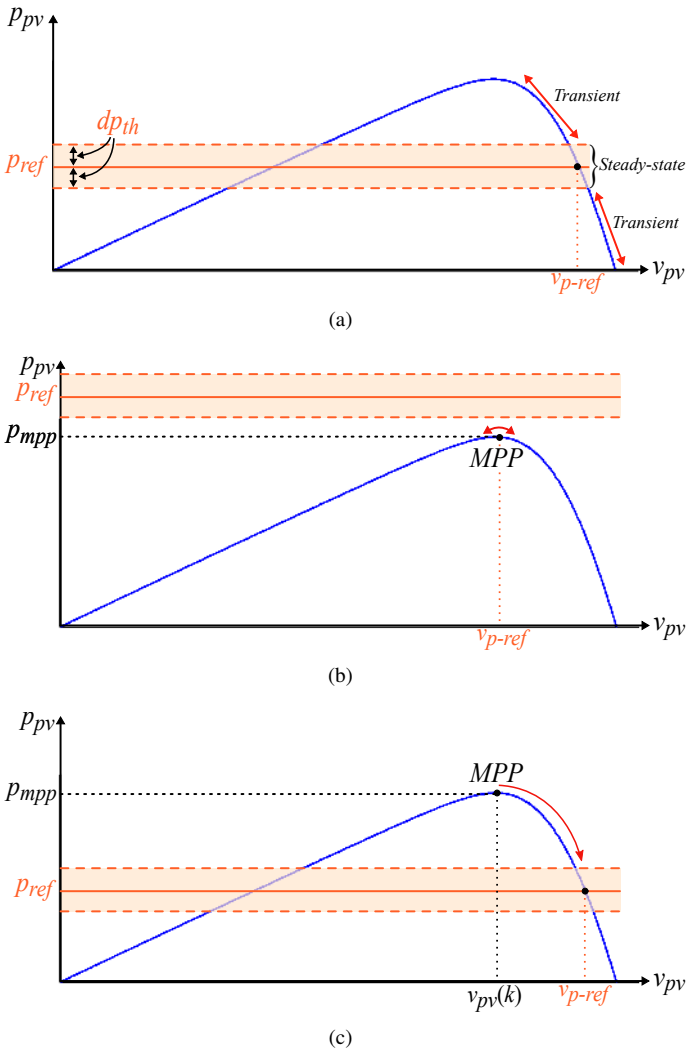

Fig. 5. The different operation modes of the PV system in constant power generation: (a) Operation at steady-state, (b) operation at MPP under steady-state, while p_{ref} is larger than the maximum available PV power, and (c) operation at MPP under transient, while p_{ref} is smaller than p_{mpp}.

A. Operation Mode Evaluation Algorithm

There are two main operational modes as depicted in Fig. 5(a). A power threshold dp_{th} is defined to distinguish between the two operation modes as:

$$\begin{cases} dp^* \leq dp_{th} & Steady\text{-}state \\ dp^* > dp_{th} & Transient \end{cases} \tag{5}$$

in which the error dp^* is defined as:

$$dp^* = p_{pv}(k) - p_{ref}, \tag{6}$$

where $p_{pv}(k)$ is the instantaneous PV power at the current calculation-step k. In steady-state, the error in (6) is close to zero, while during *transients* it can be relatively large, due to the change in the solar irradiance condition.

The implementation of the comparison in (5) can result in a wrong selection of operation mode in the condition that the PV system operates at the MPP. As illustrated in Fig. 5, this condition can happen under two circumstances:

- The controller is set to extract the maximum power from the PV system, instead of operating at FPPT. In this case, the controller sets the power reference to a value larger than the nominal maximum PV power, as depicted in Fig. 5(b).
- Due to partial shading or other reasons, the maximum available PV power (p_{mpp}) is smaller than the constant power reference during the FPPT operation. In this case, the operation mode is also similar to Fig. 5(b).

The proposed voltage reference calculation algorithm is able to calculate the MPP voltage during the above conditions. In order to achieve similar or smaller power oscillations compared to the conventional MPPT algorithms, it should be ensured that these conditions are classified as steady-state. It is known that the slope of the PV panels P-V curve (dp/dv) at MPP is close to zero. Accordingly, the absolute value of dp/dv is compared to a threshold (Thr) to identify whether the current operation point is close to the MPP. If the operation point is not close to the MPP ($|dp/dv| > Thr$), the PV system is in transient mode. It should be noted that if the current operation point is close to the MPP, two different conditions can happen:

- The power reference is larger than p_{mpp}, as illustrated in Fig. 5(b). This operation condition should be classified as steady-state. In this operation mode, dp^* is positive, as calculated from (6).
- The power reference can be smaller than p_{mpp} at the current calculation time-step. However, due to the step decrease of p_{ref}, the operation point is still at the MPP, as demonstrated in Fig. 5(c). This operation condition results in $dp^* < 0$ and should be classified as transient to achieve fast dynamics.

In order to differentiate the two conditions, the sign of dp^* is determined in the proposed algorithm, as it is shown in Fig. 4. After the detection of the operation mode, the parameter α is defined as:

$$\begin{cases} Transient & \alpha = 0 \\ Steady\text{-}state & \alpha = 1. \end{cases} \tag{7}$$

When the operation mode evaluation algorithm is implemented, it is ensured that all the operation conditions are classified correctly. The main advantage of this algorithm is to properly classify the operation at the MPP. It guarantees that the MPPT operation is classified as steady-state, which results in smaller power oscillations compared to the conventional MPPT algorithms.

B. Adaptive Voltage-Step Calculation Algorithm

The selection of voltage-step (V_{step}) is critical in the design of the FPPT algorithm. A large value of V_{step} results in fast dynamics during transients, while it generates large power oscillations in steady-state. On the other hand, with small values, relatively small power oscillations in steady-state can be achieved. However, such a choice results in slow dynamics. Thus, an adaptive voltage-step calculation algorithm is introduced in the following to improve both the dynamic and steady-state performances.

One objective of the proposed FPPT algorithm is to provide similar MPPT performance compared to conventional MPPT algorithms. In this regard, a fixed voltage-step, which is the optimal voltage-step for the MPPT operation, can be applied in the FPPT algorithm as

$$V_{step} = V_{step\text{-}b}, \tag{8}$$

in which $V_{step\text{-}b}$ is the optimal voltage-step for the MPPT operation, which can be designed by following [29]. When the fixed voltage-step $V_{step\text{-}b}$ is adopted for the FPPT algorithm, the dynamics of the system under rapidly changing environments become slow as aforementioned. Note that the change of the voltage in an FPPT operation $v_{p\text{-}ref}$ for a specific constant power reference is larger than that of the voltage changes at MPP v_{mpp} under similar environmental condition variations. This is due to the fact that the MPPT operating range is concentrated around the MPP; where the slope of the P-V curve is close to zero. Accordingly, a larger voltage-step should be applied during transients to improve the dynamics as

$$V_{step} = \overbrace{\alpha \times V_{step\text{-}b}}^{\text{Steady-state}} + \overbrace{(1-\alpha) \times V_{step\text{-}tr}}^{\text{Transient}}, \tag{9}$$

where $V_{step\text{-}tr}$ is the selected voltage-step for transient operations and it is larger than the optimal voltage-step $V_{step\text{-}b}$. During *transients*, $\alpha = 0$ and $V_{step} = V_{step\text{-}tr}$, which results in faster dynamics, while in steady-state with $\alpha = 1$, relatively low power oscillations can be achieved. Nevertheless, this algorithm still has two drawbacks:

- The FPPT operation in the right-side of the MPP with relatively small power references results in large power oscillations, even considering $V_{step\text{-}b}$ as the voltage-step, because the slope of the P-V curve (dp/dv) is large. This means smaller voltage-step values should be applied for operation points with larger dp/dv values to maintain low power oscillations.
- The dynamic transients can lead to large power deviations from the power reference (power errors). Using small voltage-step values increases the response time, as depicted in Fig. 6(a). On the other hand, by applying large voltage-step values during *transients*, the operation point may go beyond the steady-state region, in which large power oscillations are observed, as depicted in Fig. 6(b). In this case, the operation point oscillates beyond the steady-state region.

To solve these drawbacks, an adaptive voltage-step calculation algorithm is proposed as

$$V_{step} = \left(\overbrace{\alpha \times \left(1 - k_1 \frac{|dp|}{|dv|}\right)}^{\text{Steady-state}} + \overbrace{(1-\alpha) \times k_2 \times dp^*}^{\text{Transient}} \right) \times V_{step\text{-}b}, \tag{10}$$

in which α is determined by the operation mode evaluation algorithm in the previous subsection, while k_1 and k_2 are scaling factors.

During the transient operation, $\alpha = 0$, which gives $V_{step} = k_2 \times dp^* \times V_{step\text{-}b}$. In this method, the value of V_{step} depends on the error between the instantaneous power and its reference value. During transients with large errors, the voltage-step becomes large, which reduces the response time. When the PV power becomes closer to its reference value, the voltage-step becomes smaller, as illustrated in Fig. 6(c).

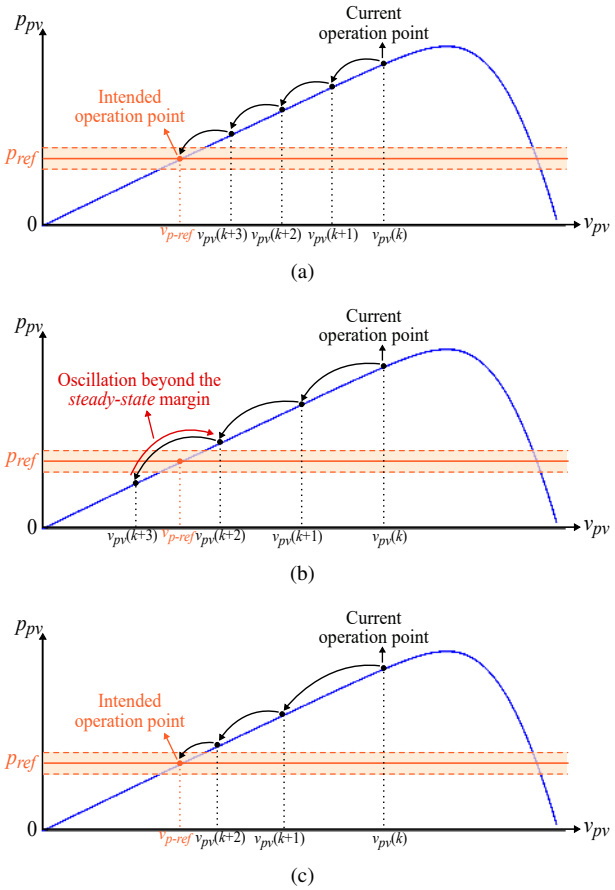

Fig. 6. Principles of the proposed voltage-step calculation algorithm during transients: (a) Constant small voltage-step, (b) constant large voltage-step, and (c) proposed adaptive voltage-step.

In steady-state, $\alpha = 1$, which results in $V_{step} = (1 - k_1|dp|/|dv|) \times V_{step\text{-}b}$. The P-V curve of the PV panels and the curve of $|dp|/|dv|$ are illustrated in Figs. 7(a) and (b). The value of $|dp|/|dv|$ is close to zero at the MPP, while it increases to relatively large values in the right-side of the MPP. The voltage-step values in the proposed algorithm are plotted in Fig. 7(c). It is seen in Fig. 7(c) that V_{step} is equal to $V_{step\text{-}b}$ at the MPP, while it is reduced to a minimum value ($V_{step\text{-}min}$) in the right-side of the MPP. Additionally, the voltage-step V_{step} remains close to a constant value in the left-side of the MPP due to the linear behavior of the P-V curve in this region. Further observations in Fig. 7(c) confirm that with the proposed algorithm, the voltage-step is adaptively modified according to the operation point of the PV panels. Therefore, the voltage oscillations can remain small in steady-state for all operation points.

C. Voltage Reference Calculation Algorithm

The voltage reference calculation algorithm for the proposed FPPT operation scheme is illustrated in Fig. 4. If the instantaneous power of the PV system is smaller than the power reference ($dp^* < 0$), a conventional P&O is applied to move the operation point towards the MPP to increase the power. If the instantaneous power is larger than the power reference, based on the intended operation region (i.e., right- or left-side of the MPP) the voltage

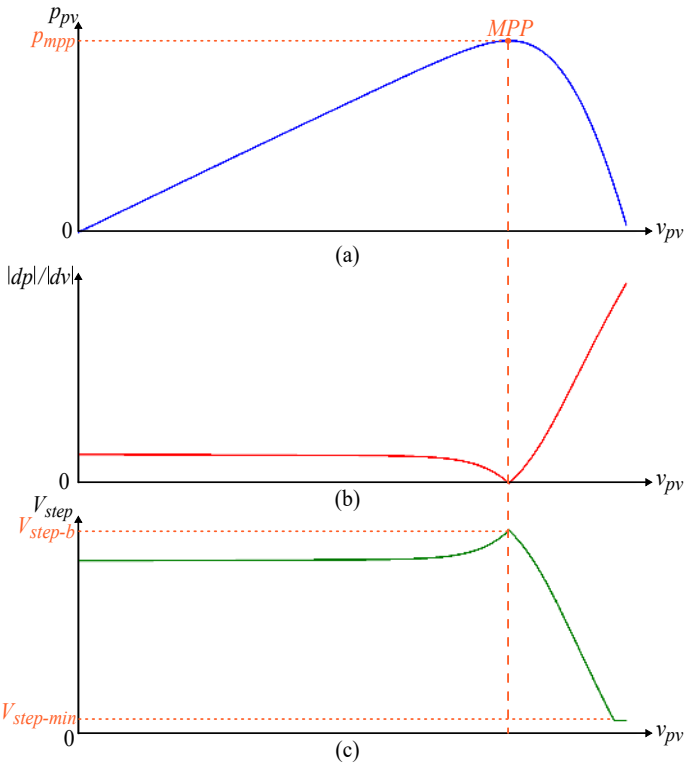

Fig. 7. Principles of the proposed voltage-step calculation algorithm in steady-state: (a) The P-V curve of the PV panels, (b) p_{pv} over v_{pv} derivation, and (c) calculated voltage-step according to (10).

reference increases or decreases, respectively. The details of the voltage reference calculation algorithm for FPPT operation can be found in [4], [5].

D. Design Guidelines

In terms of design of the proposed adaptive FPPT algorithm, the following should be considered:

- The calculation time-step (T_{step}) is selected for the optimal MPPT operation of the PV system. Notice that the proposed adaptive FPPT algorithm is able to achieve fast dynamics, even with relatively large values of time-steps. Furthermore, using the same calculation time-step in both MPPT and FPPT algorithms reduces the calculation complexity of the proposed algorithm. The sampling frequency for MPPT algorithms in commercial systems is normally $1 - 10$ Hz [30], [31].
- $V_{step\text{-}b}$ is the optimal voltage-step for the MPPT operation and can be calculated according to the available algorithms in the literature [29], [32].
- The transient voltage-step ($V_{step\text{-}tr}$) is chosen to be two to three times larger than the $V_{step\text{-}b}$ to achieve fast dynamics. Since, the slope of the P-V curve in the right-side of MPP is larger than the left-side of MPP, a smaller value can be chosen for $V_{step\text{-}tr}$ in the right-side of MPP.
- Since the proposed adaptive FPPT algorithm is based on the P&O algorithm, the effect of the intentional voltage change is considered in the selection of new voltage references. Therefore, a minimum voltage-step is required

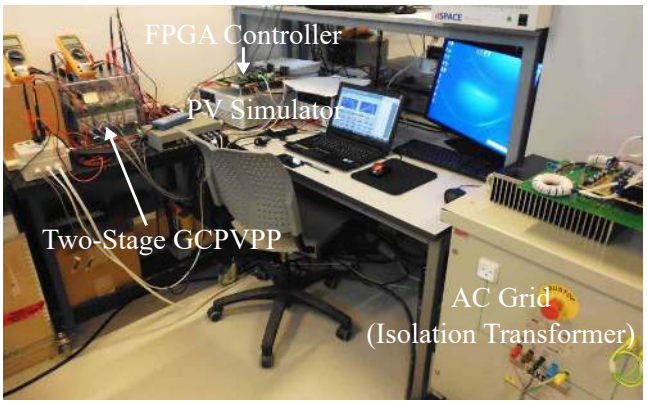

Fig. 8. Experimental setup of the 3-kVA two-stage single-phase grid-connected PV system.

in the proposed algorithm. As shown in Fig. 7(c), a minimum voltage-step ($V_{step\text{-}min}$) is applied in the proposed algorithm, which is selected according to the voltage and power rating of the PV system.

- The threshold power (dp_{th}) is chosen between 3% to 5% of the nominal power of the system.

IV. Experimental Evaluation

The operation and performance of the proposed algorithm are demonstrated experimentally using a two-stage single-phase grid-connected PV system as shown in Fig. 8. The system parameters of the experimental setup are given in Table I. The PV-side is emulated using a Chroma 62150H-1000S PV Simulator and its P-V characteristics are given in Table I. The calculation-step (T_{step}) of the proposed FPPT algorithm is selected as 1 s as a typical calculation step for commercial systems [30]. Four case studies are demonstrated in order to verify the performance of the proposed adaptive FPPT algorithm under various conditions.

The performance of the proposed adaptive voltage-step calculation algorithm is compared with the conventional voltage-step algorithms. The fixed voltage-step in (8) is referred to as *method 1* ($m1$), while the conditional voltage-step in (9) is specified as *method 2* ($m2$) and the proposed adaptive voltage-step algorithm in (10) is named *method 3* ($m3$). To obtain a numerical comparison between the performance of these algorithms, the average tracking error (in percentage of the total energy yield) during the FPPT operation is calculated. The tracking error ($T.E.$) is calculated from the difference between the actual PV output power and its reference (i.e., $|p_{pv} - p_{ref}|$), and then divided by the total energy yield as

$$T.E. = \frac{\int |p_{pv} - p_{ref}|}{\int |p_{pv}|}. \tag{11}$$

The tracking error is calculated during the FPPT period, in which the instantaneous maximum available power from the PV panels (p_{avai}) is larger or equal to the required power reference p_{ref}.

For a fair comparison of the performance of various algorithms, the following are considered: a) The rest of the control system is identical for all test conditions for different algorithms, and b) the PV emulator is used to provided similar PV curves for all test conditions.

TABLE I
PARAMETERS OF THE TWO-STAGE GRID-CONNECTED PV SYSTEM.

Parameter	Symbol	Value
PV panel maximum power*	p_{mpp}	3 kW
PV panel maximum power-point voltage*	v_{mpp}	350 V
PV panel maximum power-point current*	i_{mpp}	8.5 A
PV panel filling factor	FF	0.68
DC-bus voltage	v_{dc}	450 V
PV-side capacitor	C_{pv}	1000 μF
DC-link capacitor	C_{dc}	1100 μF
Converter switching frequency	f_{sw}	dc-dc: 16 kHz Inverter: 8 kHz
Calculation time-step	T_{step}	1 s
Optimal voltage-step for the MPPT operation*	$V_{step\text{-}b}$	2 V
Transient voltage-step	$V_{step\text{-}tr}$	Right-side: 4 V Left-side: 6 V
Voltage-step calculation parameters in right-side	k_1 k_2	0.015 0.003
Voltage-step calculation parameters in left-side	k_1 k_2	0.008 0.006
Threshold power	dp_{th}	100 W
Threshold dp/dv	$Thr.$	4 W/V

* $Irr. = 1000$ W/m^2 and $Temp. = 25^{\circ}$C.

Case I: The performance of the proposed adaptive FPPT algorithm under rapid irradiance changes with the movement of the operation point to the right-side of the MPP is evaluated in this case study and the results are presented in Fig. 9. Two test cases are demonstrated with $p_{ref} = 2$ kW and $p_{ref} = 1$ kW. Before $t = 10$ s, the irradiance is constant and the available power p_{avai} is 1 kW. A rapid increase of irradiance occurs between $t = 10$ s and $t = 25$ s, in which p_{avail} increases from 1 kW to the nominal maximum power of the PV panels, i.e., 3 kW. The output power of the PV system during the FPPT operation with the implemented voltage-step calculation algorithms under $p_{ref} = 2$ kW is illustrated in Fig. 9(a). In the results, $p_{pv\text{-}m1}$ is the PV power with *method 1*, while $p_{pv\text{-}m2}$ is the power related to *method 2* and $p_{pv\text{-}m3}$ is related to *method 3*, which is the proposed adaptive FPPT algorithm. The PV voltages related to these algorithms are shown in Fig. 9(b). A rapid decrement of the irradiance occurs between $t = 65$ s and $t = 80$ s, which reduces p_{avail} to 1 kW. The dynamic performance of *method 2* is faster than *method 1*, while the proposed adaptive FPPT algorithm (*method 3*) is the best among the three in terms of fast dynamics. The tracking error of the proposed algorithm is also smaller than other algorithms ($T.E.\text{-}m3 = 18.2\%$), as shown in Fig. 9.

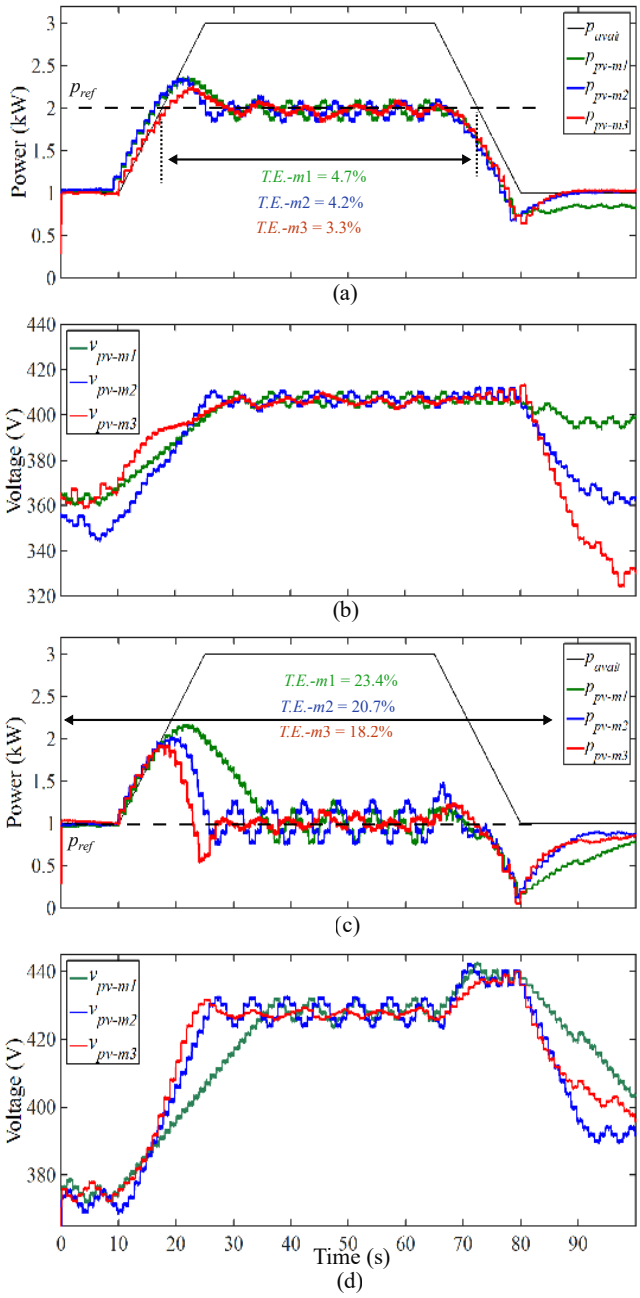

Fig. 9. Experimental results of *Case I*, i.e., FPPT operation with the movement of the operation point to the right-side of the MPP: (a) PV power with $p_{ref} = 2$ kW, (b) PV voltage with $p_{ref} = 2$ kW, (c) PV power with $p_{ref} = 1$ kW, and (d) PV voltage with $p_{ref} = 1$ kW.

The performance of the proposed algorithm operation with $p_{ref} = 1$ kW, under similar environmental conditions, is illustrated in Figs. 9(c) and (d). The proposed adaptive FPPT algorithm is able to regulate the PV power to its reference value under such rapid environmental changes. Notice that the tracking errors in this test condition are larger, compared to the test condition with $p_{ref} = 2$ kW, because of the smaller power reference in this test condition. Furthermore, the settling time of the proposed algorithm is shorter compared to the other two algorithms.

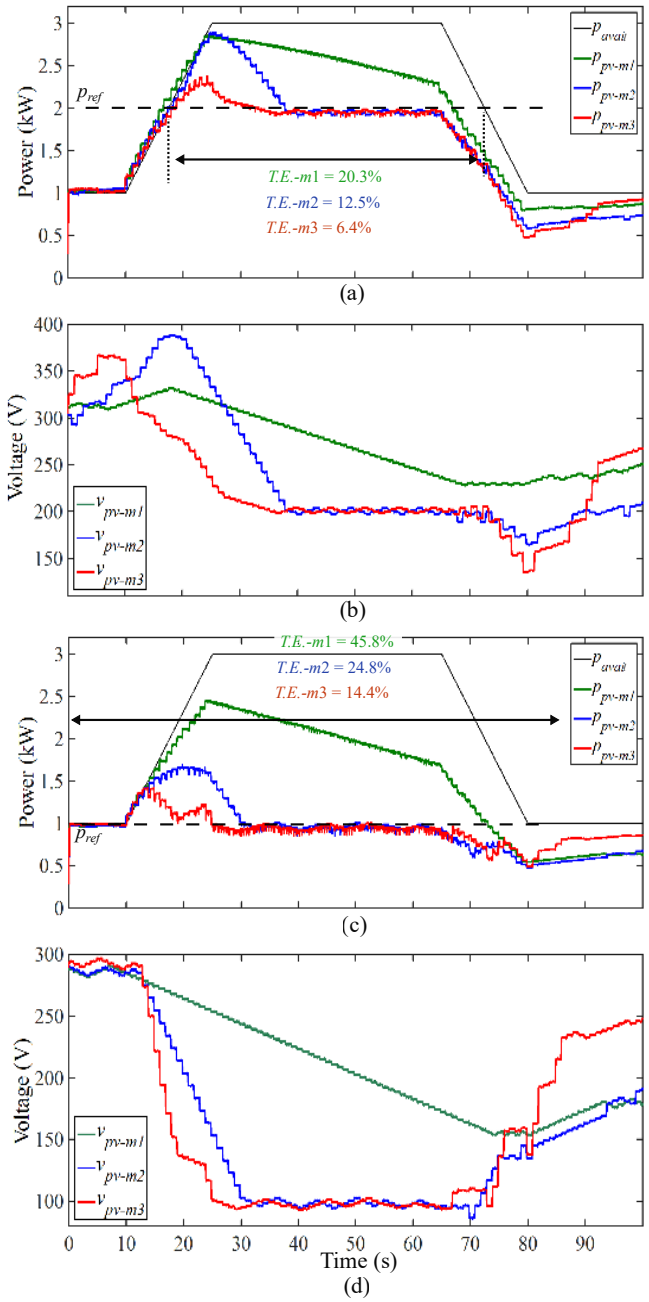

Fig. 10. Experimental results of *Case II*, i.e., FPPT operation with the movement of the operation point to the left-side of the MPP: (a) PV power with $p_{ref} = 2$ kW, (b) PV voltage with $p_{ref} = 2$ kW, (c) PV power with $p_{ref} = 1$ kW, and (d) PV voltage with $p_{ref} = 1$ kW.

Case II: The performance of the proposed FPPT algorithm for the movement of the operation point to the left-side of the MPP is investigated under similar test conditions as *Case I* and the results are illustrated in Fig. 10. The FPPT operation in the left-side of the MPP requires larger voltage adjustment under environmental changes. Therefore, the FPPT algorithm with a fixed voltage-step (*method 1*) is not able to regulate the power to its reference value under such rapid environmental changes, as depicted in Fig. 10(a) and (c). Notice that larger voltage-step values are calculated with the proposed adaptive voltage-step algorithm in Fig. 10(b) and (d), which result in a

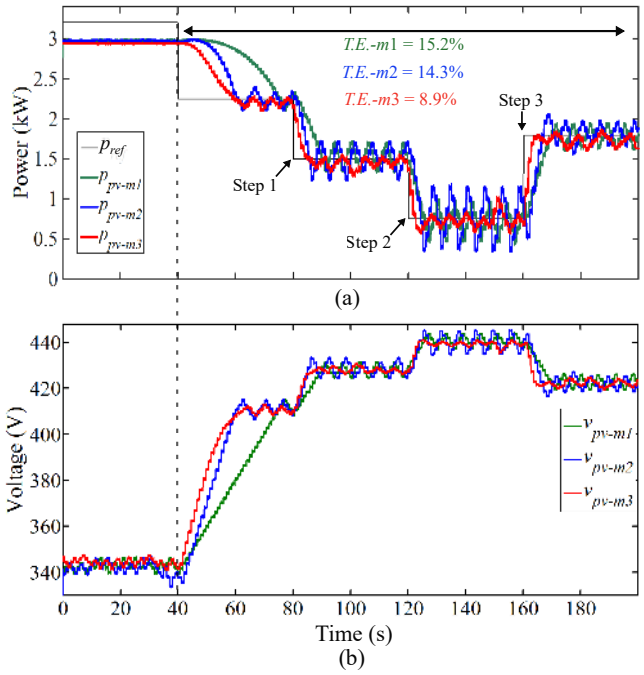

Fig. 11. Experimental results of *Case III*, i.e., FPPT operation with the movement of the voltage reference to the right-side of the MPP under changes of the constant power reference: (a) PV power, and (b) PV voltage.

fast dynamic response. Furthermore, the smaller voltage-step value in steady-state reduces the power oscillations, as observed in Fig. 10(a) and (c). The tracking error of the proposed adaptive FPPT algorithm for $p_{ref} = 1$ kW is 14.4%, which is significantly reduced compared to the tracking error for the algorithm with a fixed voltage-step ($T.E.\text{-}m1 = 45.8\%$). It is noted that *method 1* is not able to regulate the PV power to its reference during this period, while *method 2* shows a longer settling time compared to the proposed algorithm in *method 3*.

Case III: The performance of the proposed FPPT algorithm under changes of the constant power reference when moving the operation point to the right-side of the MPP is investigated in this case study and the results are presented in Fig. 11. In these tests, the irradiance is equal to $Irr = 1000$ W/m^2. Before $t = 40$ s, the central controller imposes the MPPT operation to the GCPVPP. Consequently, the proposed algorithm regulates the PV voltage to the MPP voltage, by applying a power reference, which is greater than the nominal maximum power of the PV system (i.e., $p_{ref} = 3.5$ kW), as shown in Fig. 5(b).

At $t = 40$ s, the FPPT operation with $p_{ref} = 2.2$ kW is imposed by the external controller. The power reference is reduced to 1.5 kW at $t = 60$ s, while it has a step decrease to 0.5 kW at $t = 80$ s. Finally, there is a step increase in the power reference to 1.5 kW at $t = 100$ s. The PV power with the implementation of the mentioned three methods of FPPT operation is illustrated in Fig. 11(a). The proposed adaptive FPPT algorithm (*method 3*) shows a faster dynamic response compared to the other two conventional FPPT algorithms with smaller tracking errors. The PV voltage under such conditions is depicted in Fig. 11(b), in which it can be seen that the calculated voltage-step in steady-state with the proposed adaptive voltage-step is smaller than other algorithms.

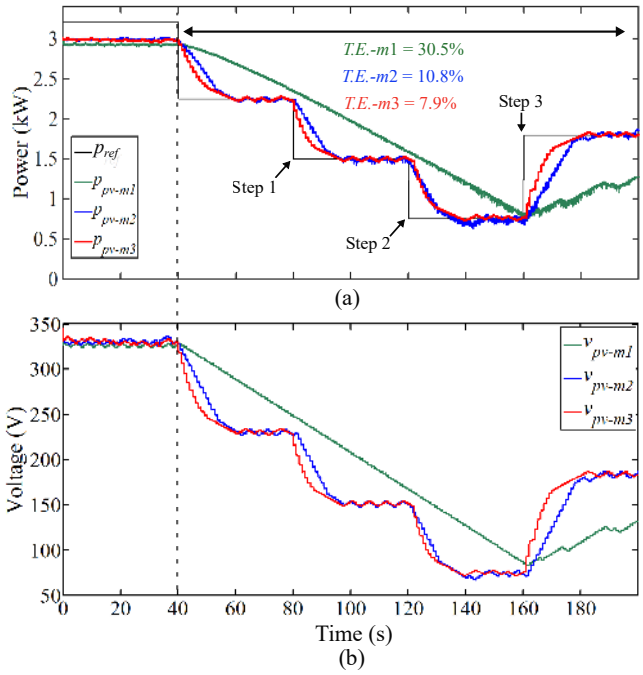

Fig. 12. Experimental results of *Case IV*, i.e., FPPT operation with the movement of the voltage reference to the left-side of the MPP under changes of the constant power reference: (a) PV power, and (b) PV voltage.

TABLE II
COMPARISON OF EXPERIMENTAL RESULTS BASED ON THE TRACKING ERROR.

Test Condition		*method 1*	*method 2*	*method 3*
Case I	$p_{ref} = 2\,kW$	4.7%	4.2%	**3.3%**
	$p_{ref} = 1\,kW$	23.4%	20.7%	**18.2%**
Case II	$p_{ref} = 2\,kW$	20.3%	12.5%	**6.4%**
	$p_{ref} = 1\,kW$	45.8%	24.8%	**14.4%**
Case III		15.2%	14.3%	**8.9%**
Case IV		30.5%	10.8%	**7.9%**

Case IV: The performance of the proposed adaptive FPPT algorithm with the movement of the operation point to the left-side of the MPP under power reference changes, similar to *Case III*, is studied and the results are illustrated in Fig. 12. It can be seen that the proposed adaptive FPPT algorithm is able to regulate the PV power to the required power reference under all operating conditions. In contrast, the other two algorithms either cannot achieve an accurate constant power generation or will have slow dynamics, as shown in Fig. 12.

Numerical comparisons of experimental results for the tracking error and settling-time are provided in Tables II and III. The tracking error of the proposed FPPT algorithm with an adaptive voltage-step is smaller compared to the obtained tracking error from the other two algorithms. Additionally, the settling time of the proposed algorithm is shorter in all of the test conditions, which proves the effectiveness of the proposed FPPT algorithm. That is, it

TABLE III
COMPARISON OF EXPERIMENTAL RESULTS BASED ON THE SETTLING TIME.

Test Condition		*method 1*	*method 2*	*method 3*
Case III	*Step 1*	8.6 s	4.9 s	**2.6 s**
	Step 2	3.2 s	3.1 s	**1.2 s**
	Step 3	8.8 s	6.1 s	**2.7 s**
Case IV	*Step 1*	*N.A.*	11.1 s	**9.0 s**
	Step 2	*N.A.*	11.2 s	**10.7 s**
	Step 3	*N.A.*	16.2 s	**10.5 s**

can achieve fast, accurate, and flexible active power tracking of grid-connected PV systems.

V. CONCLUSION

An adaptive flexible power point tracking (FPPT) algorithm for calculating the voltage reference of PV panels, which regulates the output power to a certain power reference, has been introduced in this paper. The main target of the proposed algorithm is to tackle the power system challenges (i.e., overvoltage), which may occur due to the increasing growth of the installation of GCPVPPs. Fast dynamics under rapid environmental changes were obtained by adaptively calculating the voltage-step based on the instantaneous power error. The effect of the intentional voltage reference change of the PV string on the PV power was differentiated from the effect of environmental changes by adding an extra measurement sampling in the controller. The calculation of the voltage-step according to the operation point of the PV string reduces the power oscillation during steady-state. Also, it has been shown that if the target power reference is larger than the maximum available power of the PV string, the proposed algorithm operates at the maximum power point, with performance comparable to conventional MPPT algorithms. The flexibility of the proposed adaptive FPPT algorithm has been demonstrated experimentally on a 3-kVA laboratory setup under different conditions. The tracking error of the proposed algorithm has been reduced significantly in all experimental tests, while the settling has also been decreased. The results demonstrated the applicability and effectiveness of the proposed FPPT algorithm as an additional function for existing MPPT algorithms in GCPVPPs.

REFERENCES

[1] Y. Yang, F. Blaabjerg, and Z. Zou, "Benchmarking of grid fault modes in single-phase grid-connected photovoltaic systems," *IEEE Trans. Ind. App.*, vol. 49, no. 5, pp. 2167–2176, Sep. 2013.

[2] "Technical regulation 3.2.2 for PV power plants with a power output above 11 kW," *Danish grid codes*, 2015.

[3] H. D. Tafti, A. Maswood, G. Konstantinou, J. Pou, K. Kandasamy, Z. Lim, and G. H. P. Ooi, "Study on the low-voltage ride-thorough capability of photovoltaic grid-connected neutral-point-clamped inverters with active/reactive power injection," *IET Renewable Power Generation*, vol. 11, no. 8, pp. 1182–1190, Jul. 2017.

[4] H. D. Tafti, A. I. Maswood, G. Konstantinou, J. Pou, and F. Blaabjerg, "A general constant power generation algorithm for photovoltaic systems," *IEEE Trans. Power Electron.*, vol. 33, no. 5, pp. 4088–4101, 2018.

[5] A. Sangwongwanich, Y. Yang, and F. Blaabjerg, "High-performance constant power generation in grid-connected pv systems," *IEEE Trans. Power Electron.*, vol. 31, no. 3, pp. 1822–1825, Mar. 2016.

[6] A. Sangwongwanich, Y. Yang, and F. Blaabjerg, "A sensorless power reserve control strategy for two-stage grid-connected PV systems," *IEEE Trans. Power Electron.*, vol. 32, no. 11, pp. 8559–8569, Nov. 2017.

[7] M. Chamana, B. H. Chowdhury, and F. Jahanbakhsh, "Distributed control of voltage regulating devices in the presence of high PV penetration to mitigate ramp-rate issues," *IEEE Trans. Smart Grid*, vol. 9, no. 2, pp. 1086–1095, Mar. 2018.

[8] D. Sera, L. Mathe, T. Kerekes, S. V. Spataru, and R. Teodorescu, "On the perturb-and-observe and incremental conductance MPPT methods for PV systems," *IEEE J. Photovolts*, vol. 3, no. 3, pp. 1070–1078, Jul. 2013.

[9] S. Sajadian and R. Ahmadi, "Model predictive-based maximum power point tracking for grid-tied photovoltaic applications using a Z-source inverter," *IEEE Trans. Power Electron.*, vol. 31, no. 11, pp. 7611–7620, Nov. 2016.

[10] Y. T. Jeon, H. Lee, K. A. Kim, and J. H. Park, "Least power point tracking method for photovoltaic differential power processing systems," *IEEE Trans. Power Electron.*, vol. 32, no. 3, pp. 1941–1951, Mar. 2017.

[11] S. M. R. Tousi, M. H. Moradi, N. S. Basir, and M. Nemati, "A function-based maximum power point tracking method for photovoltaic systems," *IEEE Trans. Power Electron.*, vol. 31, no. 3, pp. 2120–2128, Mar. 2016.

[12] J. H. Teng, W. H. Huang, T. A. Hsu, and C. Y. Wang, "Novel and fast maximum power point tracking for photovoltaic generation," *IEEE Trans. Ind. Electron.*, vol. 63, no. 8, pp. 4955–4966, Aug. 2016.

[13] M. A. Ghasemi, H. M. Forushani, and M. Parniani, "Partial shading detection and smooth maximum power point tracking of PV arrays under PSC," *IEEE Trans. Power Electron.*, vol. 31, no. 9, pp. 6281–6292, Sep. 2016.

[14] H. Renaudineau, F. Donatantonio, J. Fontchastagner, G. Petrone, G. Spagnuolo, J. P. Martin, and S. Pierfederici, "A PSO-based global MPPT technique for distributed PV power generation," *IEEE Trans. Ind. Electron.*, vol. 62, no. 2, pp. 1047–1058, Feb. 2015.

[15] M. Ricco, P. Manganiello, E. Monmasson, G. Petrone, and G. Spagnuolo, "FPGA-based implementation of dual kalman filter for PV MPPT applications," *IEEE Trans. Ind. Informat.*, vol. 13, no. 1, pp. 176–185, Feb. 2017.

[16] Y. Yang, F. Blaabjerg, and H. Wang, "Constant power generation of photovoltaic systems considering the distributed grid capacity," in *Proc. IEEE Applied Power Electronics Conf. and Exposition (APEC)*, Mar. 2014, pp. 379–385.

[17] Y. Yang, H. Wang, F. Blaabjerg, and T. Kerekes, "A hybrid power control concept for PV inverters with reduced thermal loading," *IEEE Trans. Power Electron.*, vol. 29, no. 12, pp. 6271–6275, Dec. 2014.

[18] A. Urtasun, P. Sanchis, and L. Marroyo, "Limiting the power generated by a photovoltaic system," in *10th Int. Multi-Conferences on Systems, Signals Devices (SSD13)*, Mar. 2013, pp. 1–6.

[19] C. Rosa, D. Vinikov, E. Romero-Cadaval, V. Pires, and J. Martins, "Low-power home PV systems with MPPT and PC control modes," in *Proc. Int. Conf.-Workshop Compatibility And Power Electronics*, Jun. 2013, pp. 58–62.

[20] A. Hoke and D. Maksimovic, "Active power control of photovoltaic power systems," in *Proc. IEEE 1st Conf. on Technologies for Sustainability (SusTech)*, Aug. 2013, pp. 70–77.

[21] R. G. Wandhare and V. Agarwal, "Precise active and reactive power control of the PV-DGS integrated with weak grid to increase PV penetration," in *Proc. IEEE 40th Photovoltaic Specialist Conf. (PVSC)*, Jun. 2014, pp. 3150–3155.

[22] C. Y. Tang, Y. T. Chen, and Y. M. Chen, "PV power system with multi-mode operation and low-voltage ride-through capability," *IEEE Trans. Ind. Electron.*, vol. 62, no. 12, pp. 7524–7533, Dec. 2015.

[23] M. Mirhosseini, J. Pou, and V. G. Agelidis, "Single- and two-stage inverter-based grid-connected photovoltaic power plants with ride-through capability under grid faults," *IEEE Trans. Sustain. Energy*, vol. 6, no. 3, pp. 1150–1159, Jul. 2015.

[24] H. D. Tafti, A. I. Maswood, Z. Lim, G. H. P. Ooi, and P. H. Raj, "NPC photovoltaic grid-connected inverter with ride-through capability under grid faults," in *Proc. IEEE 11th International Conference on Power Electronics and Drive Systems*, Jun. 2015, pp. 518–523.

[25] H. D. Tafti, A. I. Maswood, J. Pou, G. Konstantinou, and V. G. Agelidis, "An algorithm for reduction of extracted power from photovoltaic strings in grid-tied photovoltaic power plants during voltage sags," in *Proc. 42nd Annual Conf. of the IEEE Ind. Electron. Society (IECON)*, Oct. 2016, pp. 3018–3023.

[26] D. Sera, T. Kerekes, R. Teodorescu, and F. Blaabjerg, "Improved MPPT method for rapidly changing environmental conditions," in *Proc. IEEE Intern. Symposium on Ind. Electron. (ISIE)*, vol. 2, Jul. 2006, pp. 1420–1425.

[27] D. Sera, R. Teodorescu, J. Hantschel, and M. Knoll, "Optimized maximum power point tracker for fast-changing environmental conditions," *IEEE Trans. Ind. Electron.*, vol. 55, no. 7, pp. 2629–2637, Jul. 2008.

[28] G. Escobar, S. Pettersson, C. N. M. Ho, and R. Rico-Camacho, "Multisampling maximum power point tracker (MS-MPPT) to compensate irradiance and temperature changes," *IEEE Trans. Sustainable Energy*, vol. 8, no. 3, pp. 1096–1105, Jul. 2017.

[29] N. Femia, G. Petrone, G. Spagnuolo, and M. Vitelli, "Optimization of perturb and observe maximum power point tracking method," *IEEE Trans. Power Electron.*, vol. 20, no. 4, pp. 963–973, Jul. 2005.

[30] M. A. Elgendy, B. Zahawi, and D. J. Atkinson, "Assessment of perturb and observe MPPT algorithm implementation techniques for PV pumping applications," *IEEE Trans. Sustainable Energy*, vol. 3, no. 1, pp. 21–33, Jan. 2012.

[31] J. Ram, N. Rajasekar, and M. Miyatake, "Design and overview of maximum power point tracking techniques in wind and solar photovoltaic systems: A review," *Renewable and Sustainable Energy Reviews*, vol. 73, pp. 1138 – 1159, 2017.

[32] S. K. Kollimalla and M. K. Mishra, "A novel adaptive P and O MPPT algorithm considering sudden changes in the irradiance," *IEEE Trans. Energy Conversion*, vol. 29, no. 3, pp. 602–610, Sep. 2014.